2019

Enhancement of macrophage uptake via phosphatidylserine-coated acetalated dextran nanoparticles

Nishan K. Shah
University of Rhode Island

Sweta K. Gupta
University of Rhode Island

Zimeng Wang
University of Rhode Island

Samantha A. Meenach
University of Rhode Island, smeenach@uri.edu

Citation/Publisher Attribution
Shah, N. K., Gupta, S. K., Wang, Z., & Meenach, S. A. (2019). Enhancement of macrophage uptake via phosphatidylserine-coated acetalated dextran nanoparticles. *Journal of Drug Delivery Science and Technology, 50*, 57-65. doi: 10.1016/j.jddst.2019.01.013
Available at: https://doi.org/10.1016/j.jddst.2019.01.013

Enhancement of Macrophage Uptake via Phosphatidylserine-Coated Acetalated Dextran Nanoparticles

Nishan K. Shah[1], Sweta K. Gupta[2], Zimeng Wang[2], Samantha A. Meenach[1,2,*]

[1]University of Rhode Island, College of Pharmacy, Department of Biomedical and Pharmaceutical Sciences, Kingston, RI 02881

[2]University of Rhode Island, College of Engineering, Department of Chemical Engineering, Kingston, RI 02881

***Corresponding author information:**

University of Rhode Island
Department of Chemical Engineering
215A Pastore Hall
51 Lower College Road
Kingston, RI 02881
smeenach@uri.edu
Office: 401.874.4303

Fax: 401.874.4689

Abstract

Although vital to the immune system, macrophages can act as reservoirs for pathogens such as tuberculosis and human immunodeficiency virus. Limitations in the treatment of such diseases include targeting therapeutics directly to macrophages and the large systemic dosages needed. The objective of this study is to develop a nanoparticle (NP)-based drug delivery system that can provide targeted delivery into macrophages. Acetalated dextran (Ac-Dex) NP loaded with the lipophilic model compound curcumin (CUR) were synthesized and coated in 1,2-dipalmitoyl-*sn*-glycero-3-phospho-L-serine (DPPS), a phospholipid that induces phagocytosis in macrophages. DPPS-CUR NP were found to release 67.8% of encapsulated CUR within 24 hours at pH 5.35 and exhibited minimal CUR release (6.3%) at pH 7.4. DPPS-CUR NP were uptaken by murine macrophages significantly more than NP without DPPS coating and NP exposure to these macrophages resulted in minimal toxicity to the cells and minimal nitric oxide production. These results suggest that the combination of the DPPS coating and pH-sensitive polymer Ac-Dex can provide a NP delivery system capable of enhanced uptake by macrophages and potential systemic stability to more effectively deliver drugs of interest. As a result, the described DPPS-CUR NP can serve as a viable delivery system for the treatment of macrophage-associated diseases.

Keywords

Acetalated dextran; 1,2-dipalmitoyl-*sn*-glycero-3-phospho-L-serine (DPPS); macrophage-associated diseases; targeted cellular uptake; nanoparticles; drug delivery

Abbreviations

2-methoxypropene (2-MOP), acetalated dextran (Ac-Dex), curcumin (CUR), cyclic-to-acyclic ration (CAC), dichloromethane (DCM), dimethyl sulfoxide (DMSO), deionized (DI) water, 1,2-dipalmitoyl-sn-glycero-3-phosphocholine (DPPC), 1,2-dipalmitoyl-sn-glycero-3-phospho(1'-rac'glycerol) (DPPG), 1,2-dipalmitoyl-*sn*-glycero-3-phospho-L-serine (DPPS), differential scanning calorimetry (DSC), encapsulation efficiency (EE), human immunodeficiency virus (HIV), lipopolysaccharide (LPS), nitric oxide (NO), nanoparticles (NP), phosphate buffered saline (PBS), phosphatidylserine (PS), poly(vinyl alcohol) (PVA), poly(lactic-co-glycolic acid) (PLGA), p-toluenesulfonate (PPTS), scanning electron microscopy (SEM), tuberculosis (TB), transmission electron microscopy (TEM), triethylamine (TEA)

Introduction

Macrophages are vital in the removal of cellular debris and foreign bodies to maintain homeostasis in the human body [1,2], can colonize in the liver, lungs, spleen, lymph nodes, marrow, or brain, and are critical to the innate immune system [2]. An example of the importance of macrophages is in the removal of apoptotic cells via stimulation of various signals and markers that are overexpressed by presenting cells to initiate identification and engulfment [3]. Although macrophages are involved in the protection and maintenance of the human body, there are scenarios in which these cells can result in more harm than good. Macrophages have the potential to act as reservoirs for infectious pathogens, including those related to two of the most prevalent infectious diseases, tuberculosis (TB) [1,2] and the human immunodeficiency virus (HIV) [1,2]. The commonality amongst these diseases lies in the extensive treatment times and dosing regimens necessary to treat TB and HIV, often resulting in negative side effects. As a result, treatment by way of enhanced delivery to macrophages is of growing interest [1–17].

Recent progress made in the development of macrophage targeting systems have been based around receptor-ligand interactions [18]. One common approach is surface functionalization of particle systems with mannose residues to target the mannose receptor CD206), a carbohydrate-recognition domain that is largely expressed on alveolar macrophages [19,20]. In other cases, tumor associated macrophages have been targeted using peptide-based ligands such as rabies virus glycoprotein (RVG), and can be used as carriers for systems encapsulating anti-cancer therapies [21,22]. Other ligands such as 4-SO_4-GalNAc have been used to target other receptors on the surface of phagocytic macrophages to increase targeted uptake [23].

Phosphatidylserine (PS) is an anionic phospholipid that is produced and stationed on the inner membrane of healthy cells [3,5,24,25]. Once apoptosis is induced, PS transitions from the inner leaflet to the outer leaflet of the cell membrane [14]. Apoptotic cells produce a signal via PS exposure to stimulate the attraction of macrophages for engulfment of the presenting cells (phagocytosis) via receptor-ligand interactions or identification of PS binding proteins produced by phagocytes [1,3,25,26]. Although it is essential for the phagocytosis signal, there is some debate as to whether sole exposure of PS is sufficient to induce the uptake of apoptotic cells by macrophages *in vitro* [3,25,26]. However, particle-based drug delivery systems that utilize PS (specifically, 1,2-dipalmitoyl-*sn*-glycero-3-phospho-L-serine, DPPS) as the particle coating have resulted in enhanced macrophage uptake through the sole presence of PS [3], likely due to the amount of PS presented. Multiple studies centered around treatment of inflammation [7,27], HIV-1 [1,2,6,17], cancer [8,9,28], atherosclerosis [29], and MRI imaging [1,11,16] have used DPPS coatings to increase the uptake of particle-based delivery systems by macrophages or have used PS as a binding target.

Acetalated dextran (Ac-Dex) is a biodegradable, biocompatible polymer comprised of the FDA-approved excipient dextran and hydrophobic acetal groups that allow for emulsion-based NP synthesis [30–32]. Unlike commonly used drug carriers such as poly(lactic-co-glycolic acid) (PLGA), the degradation kinetics of Ac-Dex can be easily tuned by altering the ratio of cyclic to acyclic acetal groups by modifying the Ac-Dex synthesis reaction time [33,34]. The acid-sensitivity of Ac-Dex has made it a viable carrier option in applications for cancer [33–35], inflammatory-related conditions [36], vaccines [33,34], and antibiotic delivery [37]. There is a significant difference in degradation and

drug release kinetics for Ac-Dex nanoparticle (NP) systems at a pH of 5 (faster release) versus at a pH of 7.4 (slower release) [4,30,31,33–37]. Due to this difference, Ac-Dex NP systems will exhibit slower release and stability during systemic circulation (at pH 7.4) until they are delivered to a site in the body with a lower pH, such as in macrophages, where therapeutics will be readily released.

The current study involves the design of a novel therapeutic particle-based drug delivery system consisting of a phosphatidylserine (PS)-coated, polymeric (Ac-Dex), drug-loaded NP designed to enhance uptake into macrophages. The novelty of this formulation lies in the inherent ability of PS to enhance the uptake of the NP into macrophages, while the Ac-Dex core promotes burst release of the cargo directly in the macrophages owing to its acid sensitivity. Curcumin (CUR), a natural product isolated from *Curcuma longa*, was chosen as the model small molecule due to its fluorescent properties, low water solubility, and potential clinical applications [4,5,7,9,13,30,38–42].

Materials and Methods

Materials

Unless stated otherwise, materials were purchased from Sigma Aldrich (St. Louis, MO). 1,2-dipalmitoyl-sn-glycero-3-phosphocholine (DPPC), 1,2-dipalmitoyl-sn-glycero-3-phospho(1'-rac'glycerol) (DPPG), and 1,2-dipalmitoyl-*sn*-glycero-3-phospho-L-serine (sodium salt, DPPS) were purchased from Avanti Lipids (Alabaster, AL).

Synthesis and Characterization of Acetalated Dextran

Acetalated dextran (Ac-Dex) was synthesized using a previously described method [30,31]. 1 g of lyophilized dextran (9,000-11,000 MW) was dissolved in 10 mL of anhydrous DMSO with 25 mg of p-toluenesulfonate (PPTS) under nitrogen gas. The reaction was carried out for 5 minutes using 5 mL of 2-methoxypropene (2-MOP) and was quenched with 1 mL of triethylamine (TEA). The polymer was then precipitated in basic water (pH 9), filtered, lyophilized, and stored at -20°C. The cyclic-to-acyclic (CAC) ratio of Ac-Dex and acetal coverage were verified using ^{1}H NMR (Bruker 300 MHz, NMR, MA) as described previously [30,31,37].

Synthesis of PVA-Coated Nanoparticles

PVA-coated, CUR-loaded Ac-Dex NP (PVA-CUR NP) were synthesized using a single emulsion/solvent evaporation method [31]. 50 mg of Ac-Dex and 1 mg of CUR were dissolved in 1 mL of DCM. This organic solution was added to 6 mL of 3% PVA (in 1x PBS) and the resulting mixture was emulsified using a probe sonicator attached to an ultrasonic processer at 120 W and 20 kHz (Q500, Qsonica, Newtown, CT) for 1 minute with 1 second on/off pulses. The emulsion was added to 40 mL of 0.3% PVA and was spun for 4 hours to allow for organic solvent evaporation and particle hardening [30]. The spinning solution was centrifuged at 3124 x *g* for 60 minutes and particles were redispersed in a 0.1% PVA solution and frozen overnight, followed by lyophilization. PVA-coated NP without CUR (PVA-Blank NP) were formulated similarly to PVA-CUR NP by omitting CUR from the organic solutions. NP samples were stored at -20°C.

Synthesis of DPPS and DPPC-Coated Ac-Dex NP

PVA-coated NP were coated with DPPS via a film hydration method often used to make liposomal delivery systems [6,7,17,27,43,44]. DPPS was dissolved in 4 mL of chloroform and methanol (9:1 v/v) [9]. The solution was subjected to rotary evaporation using a Heidolph 2 rotary evaporator (Schwabach, Germany) to create a thin film in a 25 mL round-bottom flask. The film was dried under vacuum for 1 hour to remove excess solvent, during which the NP were washed with deionized (DI) water to remove excess PVA. The dried film containing the NP was then rehydrated with 4 mL of DI water and this solution was sonicated for 30 minutes, followed by freezing and lyophilization. After lyophilization, the resulting NP were stored at -20°C. The ratio of lipid to NP during the process was 1:5 (w/w). NP coated with DPPC and a small amount of DPPG NP were synthesized using the same method with a 5:1 (w/w) DPPC:DPPG ratio and these NP are referred to as DPPC-NP.

Nanoparticle Size and Surface Charge Characterization

Hydrodynamic diameter and surface charge of the NP were evaluated via dynamic light scattering (DLS) and zeta potential analysis, respectively, using a Malvern Nano Zetasizer (Malvern Instruments, Worcestershire, UK). The NP were diluted to 0.25 mg/mL in DI water and were analyzed at 25°C and an angle of 90°.

Evaluation of CUR NP Encapsulation Efficiency and Drug Loading

To determine the amount of CUR encapsulated in the NP systems, NP were dissolved in DMSO (1 mg/mL) and the fluorescence of the solutions was analyzed using a SpectraMax M2 Plate Reader (Molecular Devices, Sunnyville, CA) at an excitation of 420

nm and emission of 520 nm. The encapsulation efficiency (EE) and drug loading were calculated using the following equations:

$$Encapsulation\ Efficiency\ (EE) = \frac{experimental\ mass\ of\ drug\ in\ NP}{theoretical\ mass\ of\ drug\ in\ NP} x\ 100\%$$

$$Drug\ Loading = \frac{mass\ of\ drug\ in\ NP}{mass\ of\ NP}$$

Electron Microscopy Imaging Analysis of Nanoparticles

Images of the NP were taken using a Zeiss Sigma VP Field Emission-Scanning Electron Microscope (FE-SEM) (Germany) for analysis of NP morphology. After NP were suspended in basic water (15 mg/mL), 1-2 drops of this suspension were added to aluminum SEM stubs (TedPella Inc., Redding, CA), and the samples were air dried. Dried samples were then coated with a film of gold/palladium alloy using an Emscope SC400 sputter coating system at a 20 µA for 75 seconds under argon. Images of the NP systems were also captured via a JEOL JEM-2100F transmission electron microscope (TEM, Peabody, MA) for observation of the NP core and outer layers. 1 µL of 15 mg/mL NP suspension in water were placed on 200 square mesh copper grids (Election Microscopy Sciences, Hatfield, PA) and air dried prior to imaging.

Differential Scanning Calorimetry (DSC) Analysis of Nanoparticles

Thermal phase transitions of the NP systems were analyzed using differential scanning calorimetry (DSC) via a TA Q10 DSC system (TA Instruments, New Castle, DE)

connected to an RSC-90 cooling accessory. For dry-state DSC, samples were lyophilized 24 hours prior to analysis. 1-3 mg of NP were analyzed at 10°C/min from 0 to 300°C. For wet state analysis, NP were dispersed in DI water (0.1 mM DPPS) and 15 µL of the NP suspension was added to aluminum pans to be analyzed at 2°C/min and from 5 to 65°C. DSC analysis of the raw materials was also performed.

PVA Coating Quantification

Quantification of the amount of PVA on the surface of NP was completed using a previously described method [45]. NP samples were dispersed in DI water (1 mg/mL). 400 µL of sample solution, 300 µL of iodine solution (1.25 % iodine and 2.5% potassium iodide), and 1.5 mL of 4% boric acid solution were mixed together for 20 minutes at room temperature and 100 rpm. Absorbance of the samples was measured at a wavelength of 630 nm.

Phospholipid Content Quantification

Phospholipid quantification was carried out using Stewart's method [46]. Briefly, 2.7 g ferric chloride hexahydrate and 3 g of ammonium thiocyanate was dissolved in 100 mL of distilled water. NP samples were dissolved in chloroform (1 mg/mL) and were mixed with the ammonium ferrothiocyanate solution via vortexing for 5 minutes at a 2:1 (v/v) ratio. After mixing, the solution was allowed to separate, and the phospholipid content in the chloroform portion was measured via UV-vis spectroscopy at 488 nm (DPPC/G) and 452 nm (DPPS).

In Vitro Drug Release from CUR NP

Release of CUR from the NP was carried out using a previously established centrifugation technique [30]. 1 mg/mL NP samples were dispersed in PBS (pH 7.4) or sodium acetate buffer (pH 5.35) supplemented using 0.2% Tween® 80 to enhance CUR solubility. The suspensions were incubated at 37°C and 100 rpm and at predetermined time points the suspensions were removed and centrifuged at 23,102 x *g* for 15 minutes. 200 µL of the supernatant was collected and frozen at -20°C and 200 µL of fresh medium was added to the particle solution prior to re-dispersion and re-incubation. Release samples were mixed with DMSO (1:1 by volume) prior to fluorescence spectroscopy analysis at an excitation of 420 nm and emission of 520 nm [30].

Cell Culture

Murine macrophage cells (RAW 264.7) and A549 human adenocarcinoma cells obtained from American Type Culture Collection (ATCC, Manassas, VA) were used for cell culture studies. The cells were maintained at 37°C and 5% CO_2 in Dulbecco's modified Eagle's medium (DMEM) supplemented with 10% (v/v) fetal bovine serum, 100 U/ml penicillin, 100 µg/ml streptomycin, Fungizone® (0.5 µg amphotericin B, 0.41 µg/mL sodium deoxycholate), and 1 mM sodium pyruvate.

In Vitro Cytotoxicity Analysis of NP

The cytotoxic effect of the formulated NP on RAW 264.7 macrophages was determined using a resazurin assay. Cells were seeded in 96-well plate at 5,000 cells/well and incubated overnight at 37 °C and were then exposed to varying concentrations of PVA-

CUR and DPPS-CUR NP (0.001 to 0.2 mg/ml). Untreated cells were used as negative controls. After 48 hours, resazurin solution (60 μM) was added to the cells and incubated for 3 hours. The fluorescence intensity of resorufin produced by viable cells was detected at 544 nm (excitation) and 590 nm (emission) using BioTek Cytation 3 plate reader. The relative viability of each sample was calculated by:

$$Relative\ Viability\ = \frac{Sample\ Fluorescence\ Intensity}{Control\ Fluorescence\ Intensity}\ x\ 100$$

Nitrite Analysis

A Griess assay was performed to determine nitric oxide (NO) production by macrophages. Following 48-hour incubation with varying concentrations of NP (CUR-loaded and blank), 96-well plates containing the samples were centrifuged and 50 μL of the resulting supernatant was removed from each well. Griess reagents were added per manufacturer's instructions and the absorbance was measured at 550 nm. LPS (500 ng/mL), was used to promote NO production as a control.

In Vitro Cellular Uptake Via Spectroscopy and Confocal Microscopy

Cellular uptake of CUR-loaded NP by RAW 264.7 and A549 cells was observed using a Cytation 3 image reader (BioTek, Winooski, VT). Cells (7,500 cells/well) were seeded in a 96-well plate and incubated overnight at 37 °C. Cells were then incubated with 0.1 mg/ml of NP solutions and equal concentration of CUR for 1 and 3 hours. After incubation, the media was removed, and the cells were washed three times with 200 mM glycine to remove any unbound NP that were not taken up by the cells. For quantification

of cellular uptake, the fluorescence of the CUR within the cells was analyzed via fluorescence spectroscopy at 420 nm (excitation) and 520 nm (emission).

RAW 264.7 and A549 cells were seeded into 35 mm glass-bottom petri dishes at a concentration of 500,000 cells per dish and allowed to grow overnight. DPPS-CUR NP, DPPC-CUR NP, or PVA-CUR NP were suspended and bath sonicated in cell culture medium at 0.1 mg/mL and were then incubated with cells for 1 or 3 hours. Cells were washed 3x in PBS and incubated in fresh media containing CellMask Deep Red (Invitrogen) at 1 μL/mL media for 10 minutes. Cells were then fixed with 4% paraformaldehyde for 10 minutes and rinsed 3x with PBS. Fresh PBS was added and cells were immediately imaged using a Nikon Eclipse Ti2 inverted confocal fluorescent microscope.

Statistical Analysis

All measurements were performed in at least triplicate. Statistical differences for *in vitro* cellular studies was determined using one-way or two-way ANOVA with Tukey's multiple comparisons test (GraphPad Prism version 7). For cumulative drug release, Student's *t*-Test was used to determine statistical differences. A p-value of < 0.05 or lower was considered as statistically significant. Values are presented as mean $\pm$ standard deviation.

Results

Characterization of Ac-Dex Polymer and Nanoparticles

Analysis of the acetal coverage and cyclic-to-acyclic (CAC) ratio of Ac-Dex following its synthesis was confirmed via NMR. The acetal coverage of Ac-Dex was 73%, whereas the CAC ratio was 45%. PVA-coated NP were synthesized using the emulsion method to create NP with an Ac-Dex polymer core and PVA coating both with and without curcumin loading (PVA-CUR NP and PVA-Blank NP, respectively). As seen in **Table 1**, PVA-coated NP were 260-275 nm in diameter, exhibited polydispersity index (PDI) values of 0.04, and had nearly neutral surface charges (less than -3 mV), as seen from the zeta potential values.

After the synthesis of PVA-coated NP, the particles were coated with DPPS using a thin film hydration method to form DPPS-coated NP, both with and without CUR loading (DPPS-CUR NP and DPPS-Blank NP, respectively). The diameters for both the blank and CUR-loaded DPPS NP increased by approximately 75 nm in comparison to the PVA-coated NP. The PDI values were low for both DPPS NP systems (less than 0.21), however, there was a substantial decrease in zeta potential, from -3 mV (PVA-coated NP) to -40 mV (DPPS-coated NP) for both blank and CUR-loaded NP systems.

The encapsulation efficiency (EE) and drug loading (by mass) of CUR-loaded NP was analyzed to quantify the amount of CUR loaded in the particles. Both PVA- and DPPS-coated NP exhibited EE values around 25% whereas the drug loading was 7.1 and 5.2 μg CUR/mg NP for PVA-CUR NP and DPPS-CUR NP, respectively.

Morphological Analysis of NP Via Electron Microscopy

Scanning electron microscopy (SEM) and transmission electron microscopy (TEM) were used to analyze the morphology and structure of PVA- and DPPS-coated NP loaded

with CUR. SEM micrographs indicated that PVA-CUR NP presented spherical, smooth morphology and were homogenous with respect to in size (**Figure 1, top**). TEM images allowed for the visualization of a thin layer around the Ac-Dex polymer core, which likely corresponds to the PVA coating. DPPS-CUR NP were fairly monodisperse with spherical, smooth morphology as seen via SEM imaging (**Figure 1, bottom**). TEM micrographs show a coating on the Ac-Dex NP core, likely indicating the DPPS coating on the NP.

Coating Quantification

The amount of PVA and total phospholipids present in the NP formulations were quantified and are presented in **Figure 2**. There was significantly less PVA present on the DPPS and DPPC-NP in comparison to the PVA-NP ($p < 0.001$ and $p < 0.0001$, respectively). In addition, significantly more phospholipid was present in DPPS and DPPC-NP in comparison to PVA-NP ($p < 0.01$).

Differential Scanning Calorimetry (DSC) Thermal Analysis

Figure 3 shows the thermograms of the prepared NP and their corresponding raw components in their dry states. An endothermic peak at 90°C was present, indicating a bilayer phase transition for the DPPS-coated NP, which is slightly lower than the endothermic phase transition temperature of raw DPPS at 99°C. An endothermic peak was present at 187°C for raw PVA, whereas a broadened endothermic peak was present at 195°C for PVA-coated NP. Both raw CUR and Ac-Dex exhibited endothermic peaks at 177°C, signifying their melting points [30,31,37]. These prominent endothermic peaks were not present in the formulated NP. The shift from 177°C to a broad peak at 195°C for

PVA-coated NP could be due to the interaction between Ac-Dex and PVA. DPPS-coated NP exhibited a broad endothermic peak at 165°C, potentially due to the removal of the PVA and the interaction between the Ac-Dex and DPPS. For wet-state DSC analysis of the formulated NP, there were no measurable peaks present for the temperature range used; curvature corresponded to the evaporation of water.

In Vitro Drug Release from NP

The release of CUR from the particles was analyzed at two pH values, including pH 7.4 to simulate normal physiological pH and pH 5.35 to approximate the pH in macrophages [4]. Results in **Figure 4** shows that there was no significant difference in the cumulative release of CUR from PVA-coated versus DPPS-coated NP at pH 7.4 after 24 hours (5.2% vs 6.3%), signifying that the NP coating played no appreciable role in affecting CUR release at this pH. However, significantly more CUR was released at pH 5.35 for both DPPS- and PVA-coated particles (67.8% and 88.8% release at pH 5.35, respectively) in comparison to pH 7.4 ($p < 0.001$), demonstrating the sensitivity of Ac-Dex to acidic conditions. Furthermore, when comparing DPPS- and PVA-coated NP at pH 5.35, significantly more CUR was released from NP with a PVA coating, indicating the potential influence of the DPPS layer in delaying the release of the cargo ($p < 0.05$).

In Vitro Cytotoxicity Assay

The impact of the described NP systems on macrophage toxicity was evaluated and the results are presented in **Figure 5**. These results indicate that the cells exhibited relative viabilities similar to the control (media only) after 48 hours of exposure to the NP systems.

Increasing the concentration of NP imparted no significant change in the viability of cells for PVA-Blank NP, DPPS-Blank NP, or PVA-CUR NP for the concentrations tested. However, for DPPS-CUR NP there was a slight but statistically significant decrease in the viability of cells at 0.2 mg/ml in comparison to the control ($p < 0.05$).

Nitrite Analysis

Following 48-hour incubation of NP samples on cells, CUR-loaded and blank (control) NP groups produced significantly lower NO in comparison to LPS ($p < 0.0001$) (**Figure 6**). The NP groups were the same as the control group (media only) statistically, indicating little to no production of NO [47].

In Vitro Cellular Uptake

The cellular uptake of CUR-loaded NP was evaluated in RAW 264.7 macrophages and A549 adenocarcinoma cells for up to 3 hours as shown in **Figure 6**. Exploiting the fluorescent properties of CUR, the presence of CUR-loaded NP within cells can easily be detected via fluorescence imaging and spectroscopy. After 1 hour of exposure, significantly more DPPS-coated NP were uptaken by macrophages and A549 cells in comparison to PVA-coated NP, DPPC-coated NP, and raw CUR ($p < 0.0001$). For both cell types and all formulations, uptake was not statistically different between 1 and 3-hour exposures. In addition, significantly more NP were uptaken in RAW macrophages in comparison to A549 cells for all NP formulations. Confocal microscopy confirmed fluorescence spectroscopy quantification, showing higher fluorescence in macrophages in comparison to A549 cells, indicating increased NP uptake. In addition, more NP were uptaken in DPPS-

coated NP in comparison to DPPC- and PVA-coated systems in RAW and A549 cells. Images indicate that CUR-loaded NP were primarily uptaken into the cytoplasm of macrophages, especially for DPPS-CUR NP. On the other hand, there were minimal NP located in the cytoplasm of A549 cells; instead the NP were more readily located in the cellular membranes.

Discussion

Nanoparticle Design and Analysis

The use of Ac-Dex as a biodegradable NP core for drug delivery can allow for a system with tunable and/or triggered degradation [32]. For the described NP systems, the acetal coverage of Ac-Dex was similar to previous studies [30,31,37], whereas the CAC ratio was slightly lower. The resulting Ac-Dex was favorable for the given application as the adequate acetal coverage imparts hydrophobicity to Ac-Dex, allowing for NP formulation and the lower CAC ratio will allow for faster drug release at acidic pH [30,31,35,37].

The increase in diameter and PDI from PVA-coated NP to DPPS-coated NP is likely due to the presence of the DPPS coating around the Ac-Dex core. It has been shown that an increase in NP diameter can lead to an increase in the uptake of NP into macrophages, where particles 200 nm in diameter or greater are often subjected to a greater amount of macrophage uptake [48–50]. For this study, larger NP were desired and successfully formed (up to 350 nm for DPPS-coated NP), which was advantageous since increased macrophage uptake was an objective [4]. While DPPS-coated NP exhibited

418 higher PDI values then PVA-coated NP, these values were still low, indicating that all of
419 the formulated NP systems were homogenous with respect to size.

420 The surface charge of the NP, as indicated by zeta potential, decreased significantly
421 (from -3 to -40 mV) upon coating with DPPS. The negative surface charge on the DPPS-
422 loaded NP is indicative of the polar head of DPPS being exposed to the outer environment,
423 similar to how apoptotic cells present DPPS to the outer leaflet of cells prior to engulfment
424 by macrophages [6,28]. The highly negatively surface charge is significantly lower than
425 the -25 mV threshold of being functionally negative, indicating that the NP are less likely
426 to aggregate due to electrostatic repulsion [51,52]. It should be noted that DPPC-coated NP
427 were also lower than the -25 mV threshold, indicating a functionally negative charge. In
428 addition, there were no differences in size, PDI value, or zeta potential upon the loading of
429 CUR on the NP core, indicating that the loading of the model drug had no significant effect
430 on the particle systems with respect to these characteristics.

431 CUR was encapsulated in the NP for two purposes: 1) to provide a model small
432 molecule that is easy to encapsulate owing to its hydrophobicity and 2) the inherent
433 fluorescence of CUR within the NP allows for easy fluorescence imaging and detection.
434 The encapsulation efficiency (EE) of CUR in the NP was lower than previously reported
435 values, which have ranged from 50-88% [7,9,38]. However, since CUR was used as a
436 model small molecule, the EE values were satisfactory for this study. Upon coating the NP
437 with DPPS, CUR loading decreased slightly but the encapsulation efficiency stayed the
438 same, indicating that the DPPS coating did not significantly affect CUR loading.

439 The SEM and TEM micrographs indicate that the particles are spherical in shape
440 and monodisperse, which correlates to the PDI values for the systems. The DPPS-CUR NP

seem to have slightly more coating on the NP surfaces, which could be due to the increased presence of DPPS.

Coating Quantification

DPPS was selected to coat the nanoparticles owing to its ability to stimulate an "eat-me" signal on apoptotic cells [1,3,11,16,17]. For cell studies, DPPC-NP were produced as a control lipid system. Initially, the NP systems were coated with PVA because it is one of the most widely used polymers in the pharmaceutical industry [45] and has been extensively used as a NP coating agent due to the steric effects PVA coating imparts on NP, inhibiting aggregation. During the synthesis of phospholipid-coated NP, a significant portion of the PVA was washed away prior to phospholipid coating, since there is significantly less PVA present on phospholipid-coated NP in comparison to PVA NP (**Figure 2**). It is also likely that the phospholipid coating shielded the remaining PVA upon adsorption to the NP surface, as indicated by the low mass presence of PVA on phospholipid-coated NP the high mass presence of total phospholipid on the NP, and the changes in surface charge (**Figure 2**).

Thermal Analysis of Nanoparticle Formulations

Dry-state DSC thermograms indicated the presence of DPPS in the DPPS-coated NP via the bilayer phase transition peak that occurred at 90°C for the NP, which is slightly lower than the raw DPPS endothermic peak present at 99°C. This transition signifies the presence of bilayer formation of the phospholipid around the Ac-Dex polymer core in its dry state. The decrease in the transition temperature is likely due to the interaction of the

multiple components in the formulation. As the transition temperatures of the NP formulations were just below or well above 100°C, they are likely to be stable in the dry state and can be easily reconstituted before use [53]. The endothermic peak that raw CUR exhibited at 177°C was not observed in CUR-loaded NP. According to our previous research (data not shown), this is likely due a limitation in DSC detection with relation to the actual amount of CUR in the samples.

In studies using liposomal formulations, DSC is used to assess the transition temperature(s) in the systems in order to determine the presence and state of bilayers and the differences associated between blank liposomes and modified/drug-loaded systems [43,44]. For wet-state analysis (**Figure 3C)**, there was no endothermic peak present around 50-60°C, which is the temperature at which the gel/crystalline phase transition occurs for PS bilayers in aqueous solutions [24,54]. Such a phenomenon could have occurred based on the preparation method used, as described previously. In certain cases, self-assembly of polymer-lipid structures can occur via hydrophobic interaction between the lipid tails and a polymeric core simultaneously with hydrophilic interactions between the polar head and external environment [55]. Due to the concentration dependency of DSC, it is more likely that the DPPS concentration may have been too low to be detectable by thermal analysis, like that of the CUR detection limit mentioned previously. It should be noted that the curvature of the thermograms in **Figure 3C** corresponds to the evaporation of water, which is not shown in the thermogram. Overall, the results indicate the presence of DPPS on the surface of the NP, further strengthening what has been previously described with respect to successful DPPS coating of the described systems.

Curcumin Release from Nanoparticles

The release from CUR from PVA- and DPPS-coated NP was evaluated to demonstrate the ability of the system to provide sustained release of a therapeutic agent and to show the acid-sensitive nature of Ac-Dex. Ac-Dex is known to degrade more quickly in acidic environments [32]. In a previous study, Ac-Dex particles released 60% of their camptothecin payload after 7 days [35] and 15% of rapamycin after 10 days [4] at pH of 7.4. Comparatively, at pH values of 5 or lower, Ac-Dex particles released 100% of their content in as little as 24 hours [4,30,33]. For this study, at pH 5.35, 9.3% of CUR was initially released from DPPS-CUR NP and 29.2% was released after 1 hour, followed by a sustained release of cargo of 67.8% after 24 hours, when equilibrium is reached. At pH 7.4, both NP systems exhibited minimal CUR release, demonstrating the stability of Ac-Dex in neutral pH. However, both systems exhibited triggered release at pH 5.35, exhibiting a significantly higher total release in comparison to their pH 7.4 counterparts ($p < 0.001$). Overall, these data indicate a more stable NP formulation at pH 7.4 and the potential for triggered release at pH 5.35, corresponding to stability in circulation and burst release in macrophages, respectively.

Cytotoxic Analysis and Macrophage Uptake of Nanoparticles

To assess the *in vitro* cytotoxicity of the NP formulations on RAW 264.7 macrophages, the cells were exposed to the systems for 48 hours. It was observed that the NP systems were not toxic to the cells, however, a slight, but significant, decrease in viability of RAW 264.7 cells for DPPS-CUR NP at 0.2 mg/ml was observed (**Figure 5**). This decrease in viability was minimal and could easily be overcome by using lower

concentrations of the particles in future studies. Overall, these results indicate the safety of the described NP for a time period longer than necessary for NP uptake into macrophages, indicating that they are safe to use in the intended fashion.

Nanomaterials may provoke immune and inflammation responses following interactions with multiple biological entities [49]. To assess inflammatory and immune response stimulation, NO production was measured using a Griess assay, where LPS was used as a positive control to stimulate NO production in RAW macrophages. It was observed that NP at varying concentrations stimulated significantly less NO production in comparison to LPS and resulted in NO concentrations comparable to that of the control (media only). Results indicated that blank NP caused NO production at concentrations similar to that of the CUR-loaded NP. These data indicate both blank and CUR-loaded formulations produced minimal NO and that CUR did not play an active role in the inhibition of NO production.

Since the purpose of this study was to formulate acid-sensitive NP capable of enhanced macrophage uptake, the ability of DPPS-coated NP to be uptaken by macrophages was evaluated, with A549 cells acting as control tissue. PVA and DPPC-coated NP were used as other coatings for comparison to DPPS. Several environmental and physicochemical factors are known to influence the cellular uptake of NP into macrophages. The preferential uptake of DPPS-CUR NP by macrophages in comparison to PVA-CUR NP and DPPC-CUR NP is likely due to the DPPS coating on the Ac-Dex polymeric core. Confocal microscopy in tandem with fluorescence quantification of CUR-loaded NP within the cells confirm the uptake of DPPS-CUR-NP and localization to the cytoplasm of macrophages. The presence of DPPS on the cellular surface is known to cause

533 an “eat-me” signal in cells that are transitioning toward an apoptotic state, causing
534 macrophages to identify and phagocytose the dying cells [1–3,7,11]. Therefore, in terms of
535 recognition, the DPPS coating on the Ac-Dex NP was identified by the macrophages,
536 which produced the necessary phagocytotic action, resulting in cellular uptake of the
537 particles [1,6,7,16,25,27]. In most cases, apoptosis is initiated by the presence DPPS and
538 other signaling pathways such as receptor-ligand interactions or identification of PS
539 binding proteins produced by phagocytes. However, there is a debate as to whether DPPS
540 recognition by itself is sufficient for the uptake of apoptotic cells by phagocytotic cells
541 [3,25]. In the case of nanoparticles, is has been shown that a DPPS coating alone is
542 sufficient for uptake, as seen in this current study and otherwise [7,16,17].

543 Another consideration for cellular uptake of the described particles is in terms of
544 their physicochemical characteristics. Stimulation of phagocytosis of nanoparticle-based
545 delivery systems via macrophages is also dependent on the size and shape of the particles.
546 Since the DPPS-CUR NP were greater than 300 nm in diameter, it is likely that these NP
547 were phagocytosed not only because of the DPPS layer, but also because of their size
548 [4,48,56]. It is well known that surface charge can play a role in biological interactions.
549 Interestingly, surface charge did not play a role in the uptake of the NP, as shown by the
550 similar charges of DPPC and DPPS-coated NP that produced significantly different uptake
551 quantities [48,51,52]. This phenomenon could also explain the minimal phagocytosis of
552 the PVA-coated NP and confirm the effect of DPPS on the uptake of the NP. Overall, the
553 results indicate the successful uptake of DPPS-coated NP into macrophages, indicating that
554 these systems could be used for the treatment of a multitude of diseases involving infected
555 cells.

Conclusions

Macrophages can harbor infectious agents that lead to potentially fatal diseases such as TB and HIV. Due to this, treatment of these diseases is challenging and therefore, the goal of this study was to design a delivery system that would enhance the uptake of nanoparticles into macrophages, allowing for targeted delivery, a decrease of systemic side effects, and decreased treatment times. Results showed that both PVA-coated and DPPS-coated NP were monodisperse and that there was a significant increase in size upon DPPS coating. The surface charge of the DPPS NP was -40 mV, indicating that DPPS was present on the surface of the NP. This was further confirmed via PVA quantification, which indicated minimal amounts of PVA on the DPPS NP. DSC results confirmed the presence of a DPPS bilayer on the NP surface and the likely stability of the NP during synthesis and storage conditions. CUR-loaded NP successfully encapsulated CUR and this agent was more quickly released in acidic conditions in comparison to neutral pH owing to the acid sensitivity of Ac-Dex. In addition, CUR-loaded NP exhibited sustained release of CUR. PVA-coated NP were not readily phagocytosed by macrophages, whereas DPPS-coated NP were phagocytosed within 1 hour of exposure, showing the physiological relevance of the DPPS coating for the enhanced delivery to macrophages. These data show that the particles can potentially deliver therapeutic agents throughout the body with fewer concerns of systemic drug exposure, and when exposed to macrophages, the particles are capable of being phagocytosed relatively quickly. Therefore, the combination of Ac-Dex and DPPS can be a viable option for targeted delivery for macrophage-associated diseases.

Conflicts of Interest

The authors have no conflicts of interest to report for this study.

Acknowledgements

The authors thank Dr. Richard Kingsley for assistance with TEM imaging, Mitch Gravely for confocal imaging, and RIN^2 for SEM, TEM, and DSC access. Research reported in this publication was partially supported by the Institutional Development Award (IDeA) Network for Biomedical Research Excellence from the National Institute of General Medical Sciences of the National Institutes of Health under grant number P20GM103430. In addition, this work was made possible by the use of equipment and services available through the RI-INBRE Centralized Research Core Facility. This material is based upon work conducted at a Rhode Island NSF EPSCoR research facility, supported in part by the National Science Foundation EPSCoR Cooperative Agreement #EPS-1004057. This material is also based in part upon work supported by the National Science Foundation under grant #1508868. Any opinions, findings, and conclusions or recommendations expressed in this material are those of the authors and do not necessarily reflect the view of the National Science Foundation or National Institutes of Health.

Tables and Figures

Table 1. Diameter, polydispersity index (PDI), surface charge via zeta potential, curcumin encapsulation efficiency, and drug loading of nanoparticle systems.

	Diameter (nm)	PDI	Zeta Potential (mV)	Encapsulation Efficiency (%)	Drug loading (µg drug/mg particle)
PVA-Blank NP	262.6 ± 1.9	0.04 ± 0.00	-2.2 ± 3.5	---	---
PVA-CUR NP	272.6 ± 10.4	0.04 ± 0.01	-3.0 ± 0.6	25.1 ± 0.1	7.1 ± 1.8
DPPS-Blank NP	335.6 ± 3.8	0.21 ± 0.43	-40.4 ± 3.3	---	---
DPPS-CUR NP	350.5 ± 16.9	0.13 ± 0.65	-40.6 ± 1.3	24.5 ± 0.1	5.2 ± 0.7

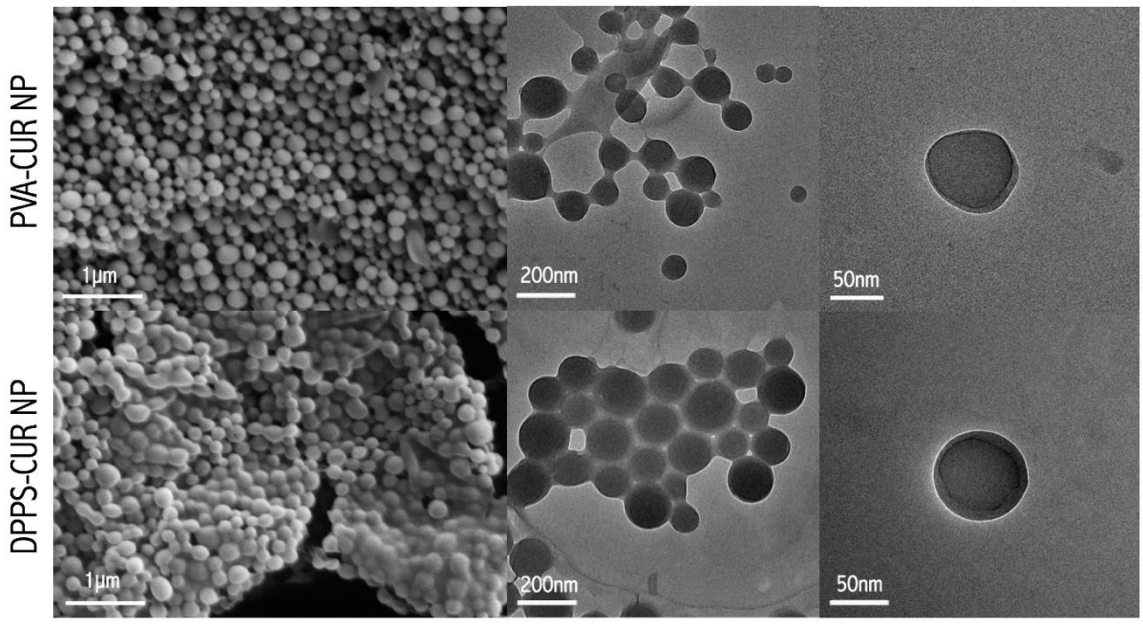

Figure 1. Representative SEM (left) and TEM (middle, right) micrographs of PVA- and DPPS-coated, CUR-loaded nanoparticles (PVA-CUR NP and PVA-DPPS NP, respectively).

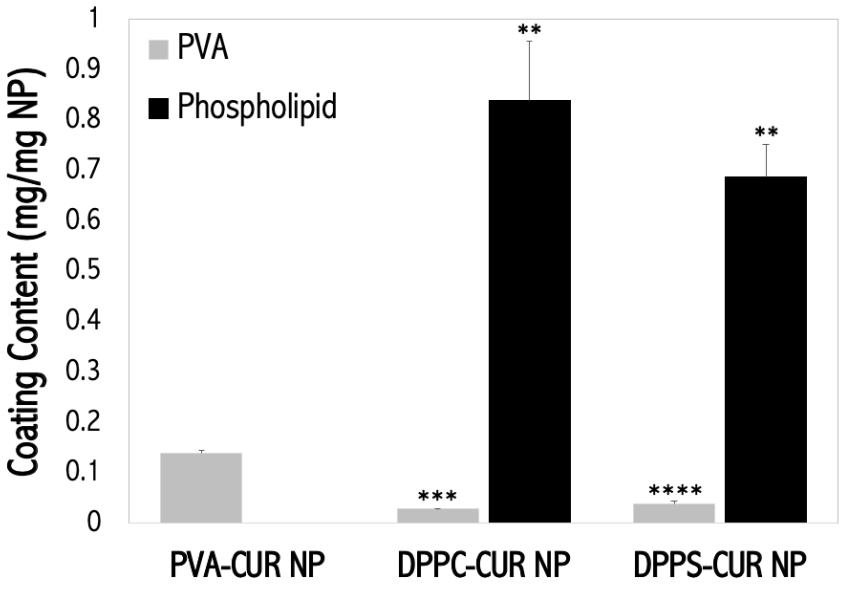

609

610 **Figure 2**. Quantification of the amount of poly(vinyl alcohol) (PVA) and total

611 phospholipid in PVA-CUR, DPPC-CUR, and DPPS-CUR nanoparticles (NP) (* $p < 0.05$,

612 **$p < 0.01$,***$p < 0.001$ in comparison to PVA-CUR NP).

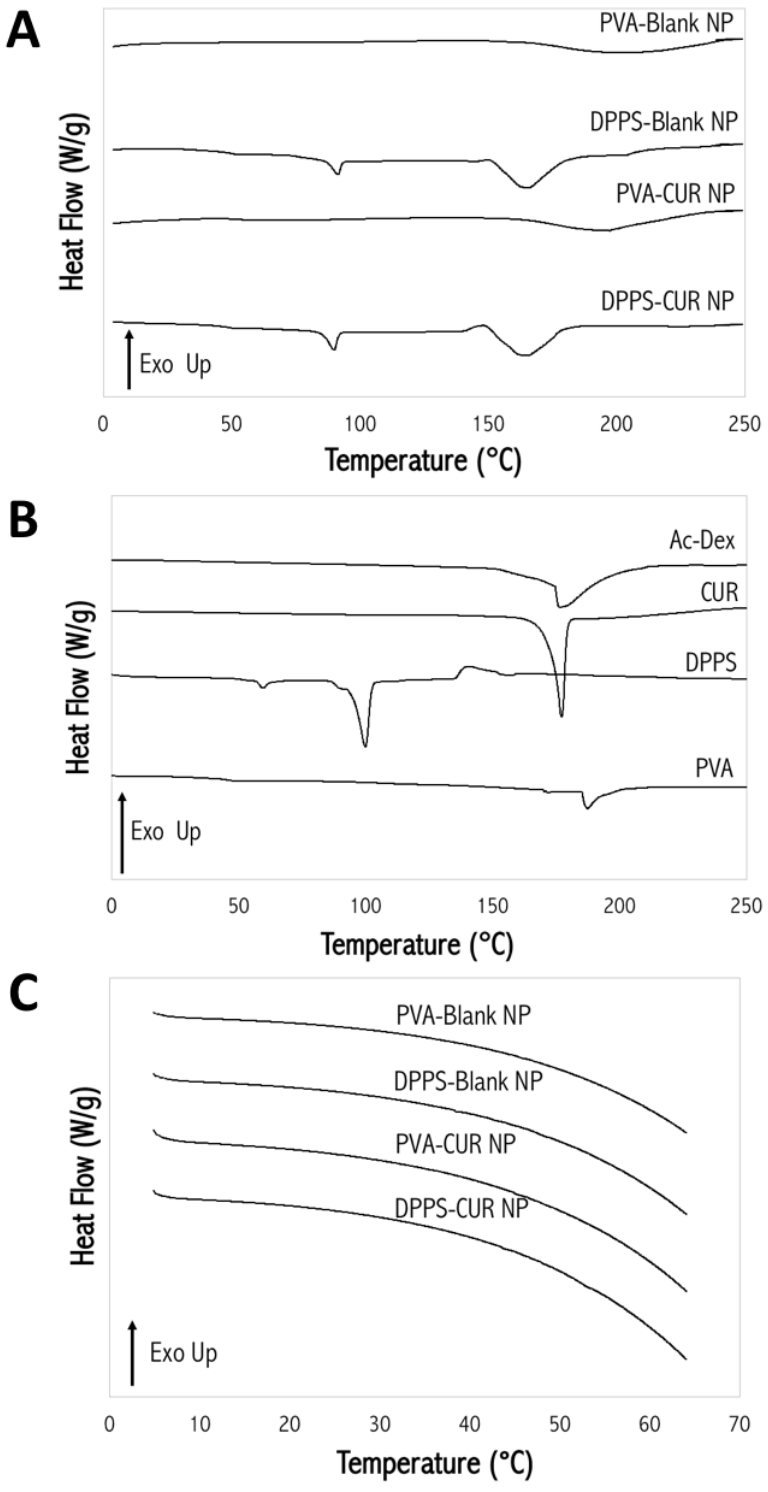

Figure 3. Differential scanning calorimetry (DSC) thermograms of: (A) formulated nanoparticles and (B) the raw components that make up the nanoparticle systems in their dry state, and (C) formulated nanoparticles in their wet state.

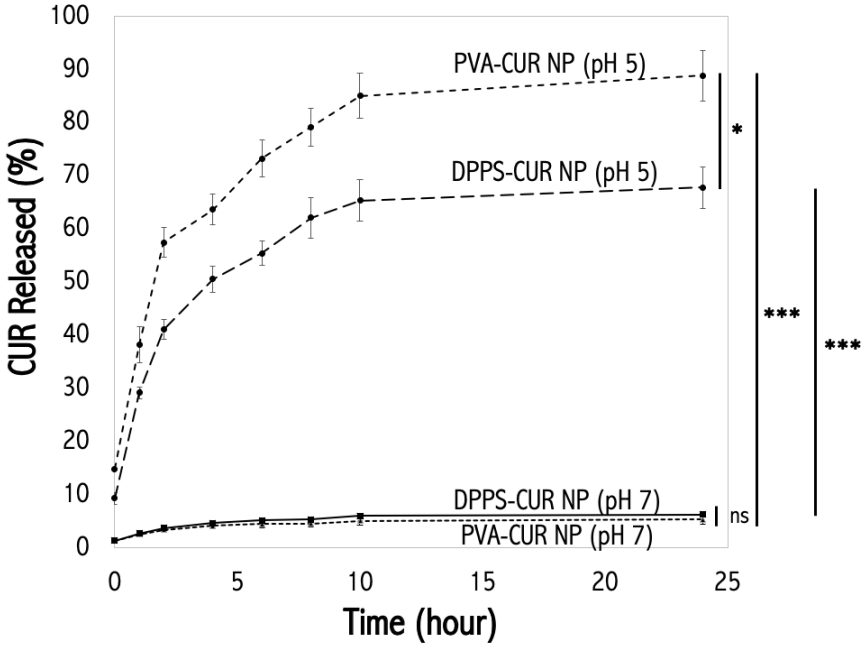

617

618 **Figure 4**. Cumulative release of curcumin (CUR) from nanoparticle systems at pH 7 and

619 pH 5 (*p < 0.05, **p < 0.01, ***p < 0.001, ns = non-significant).

620

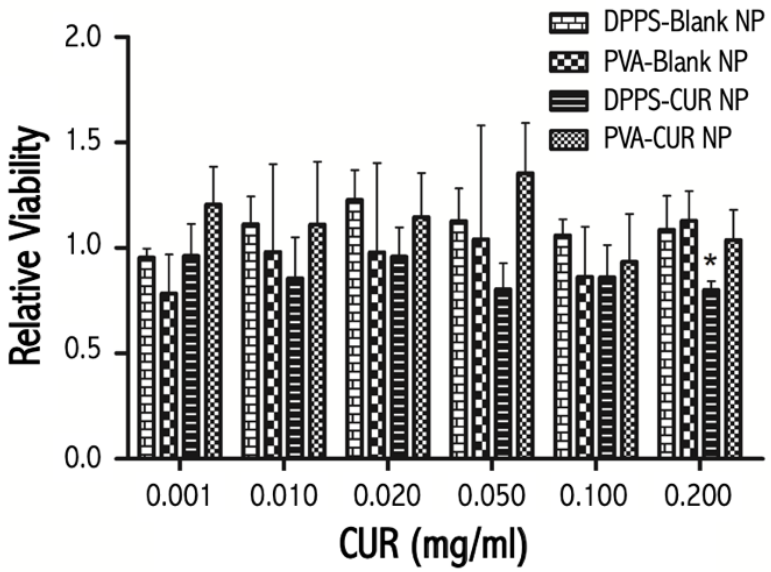

621

622 **Figure 5**. Cytotoxicity analysis (relative viability) of nanoparticle systems on RAW

623 264.7 macrophages after 48 hours of exposure compared to control (*p < 0.05).

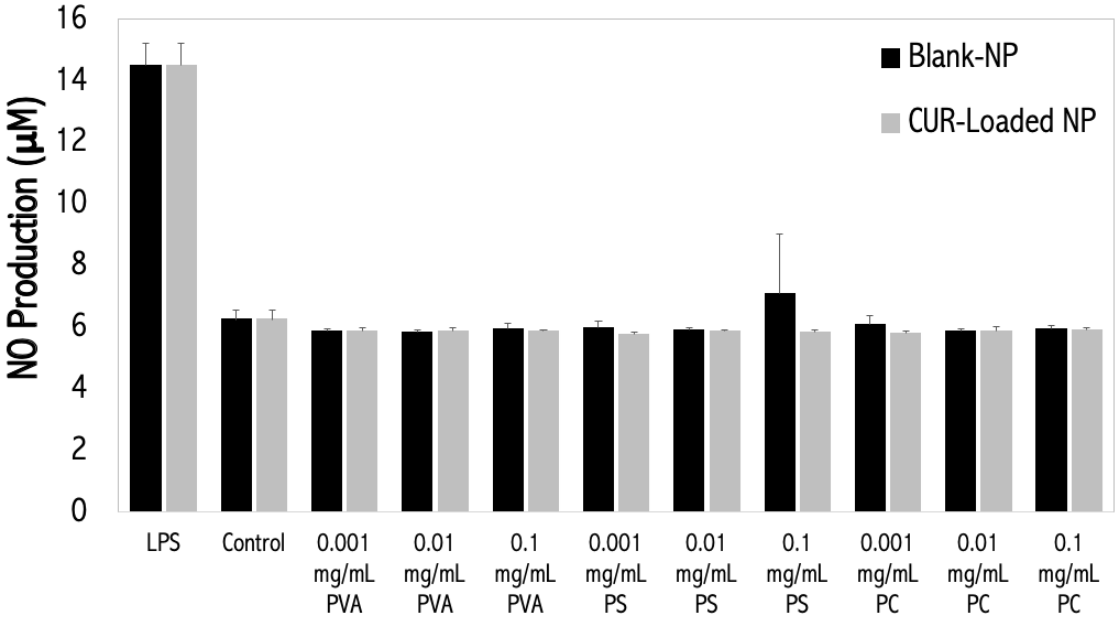

624

625 **Figure 6.** Nitric oxide (NO) production from RAW 264.7 macrophages incubated for 48
626 hours with varying concentrations of nanoparticle formulations or LPS. No statistical
627 significance was observed between the groups and control group (no treatment) and all
628 were statistically lower than the LPS sample ($p < 0.0001$).

629

630

631

632

633

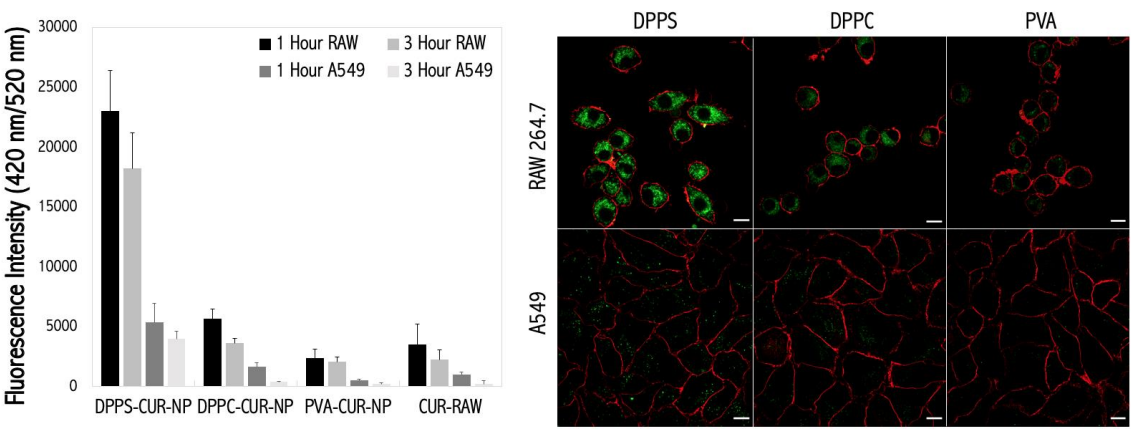

634

635 **Figure 7.** (Left) Fluorescence spectroscopy analysis of nanoparticle uptake into cells and

636 (Right) representative confocal images of nanoparticle uptake by RAW 264.7 macrophages

637 and A549 cells (scale bar = 10 μm).

638

639

640

641

642

643

644

645

646

647

648

649

650

651

652

653 **References**

654 [1] V. Bagalkot, J.A. Deiuliis, S. Rajagopalan, A. Maiseyeu, “Eat me” imaging and
655 therapy, Adv. Drug Deliv. Rev. 99 (2016) 2–11. doi:10.1016/j.addr.2016.01.009.

656 [2] F. Ahsan, I.P. Rivas, M.A. Khan, A.I. Torres Suárez, Targeting to macrophages:
657 Role of physicochemical properties of particulate carriers - Liposomes and
658 microspheres - On the phagocytosis by macrophages, J. Control. Release. 79
659 (2002) 29–40. doi:10.1016/S0168-3659(01)00549-1.

660 [3] K.S. Ravichandran, Beginnings of a Good Apoptotic Meal: The Find-Me and Eat-
661 Me Signaling Pathways, Immunity. 35 (2011) 445–455.
662 doi:10.1016/j.immuni.2011.09.004.

663 [4] K.J. Kauffman, N. Kanthamneni, S.A. Meenach, B.C. Pierson, E.M. Bachelder,
664 K.M. Ainslie, Optimization of rapamycin-loaded acetalated dextran microparticles
665 for immunosuppression, Int. J. Pharm. 422 (2012) 356–363.
666 doi:10.1016/j.ijpharm.2011.10.034.

667 [5] A. Matsumoto, Y. Takahashi, M. Nishikawa, K. Sano, M. Morishita, C.
668 Charoenviriyakul, H. Saji, Y. Takakura, Role of Phosphatidylserine-Derived
669 Negative Surface Charges in the Recognition and Uptake of Intravenously Injected
670 B16BL6-Derived Exosomes by Macrophages, J. Pharm. Sci. 106 (2016) 168–175.
671 doi:10.1016/j.xphs.2016.07.022.

672 [6] R.A. Petazzi, A. Gramatica, A. Herrmann, S. Chiantia, Time-controlled
673 phagocytosis of asymmetric liposomes: Application to phosphatidylserine
674 immunoliposomes binding HIV-1 virus-like particles, Nanomedicine

675 Nanotechnology, Biol. Med. 11 (2015) 1985–1992.
676 doi:10.1016/j.nano.2015.06.004.
677 [7] J. Wang, Y.-X. Kang, W. Pan, W. Lei, B. Feng, X.-J. Wang, Enhancement of Anti-
678 Inflammatory Activity of Curcumin Using Phosphatidylserine-Containing
679 Nanoparticles in Cultured Macrophages, Int. J. Mol. Sci. 17 (2016) 969.
680 doi:10.3390/ijms17060969.
681 [8] L. Zhang, H. Zhou, O. Belzile, P. Thorpe, D. Zhao, Phosphatidylserine-targeted
682 bimodal liposomal nanoparticles for in vivo imaging of breast cancer in mice, J.
683 Control. Release. 183 (2014) 114–123. doi:10.1016/j.jconrel.2014.03.043.
684 [9] Y. Zheng, Y. Chen, L. Jin, H. Ye, G. Liu, Cytotoxicity and Genotoxicity in Human
685 Embryonic Kidney Cells Exposed to Surface Modify Chitosan Nanoparticles
686 Loaded with Curcumin, AAPS PharmSciTech. (2015). doi:10.1208/s12249-015-
687 0471-1.
688 [10] J. Van Ingen, R.E. Aarnoutse, P.R. Donald, A.H. Diacon, R. Dawson, G. Plemper
689 Van Balen, S.H. Gillespie, M.J. Boeree, Why do we use 600 mg of rifampicin in
690 tuberculosis treatment?, Clin. Infect. Dis. 52 (2011). doi:10.1093/cid/cir184.
691 [11] V. Bagalkot, M.A. Badgeley, T. Kampfrath, J.A. Deiuliis, S. Rajagopalan, A.
692 Maiseyeu, Hybrid nanoparticles improve targeting to inflammatory macrophages
693 through phagocytic signals, J. Control. Release. 217 (2015) 243–255.
694 doi:10.1016/j.jconrel.2015.09.027.
695 [12] S.H.M. Chachuli, A. Nawaz, K. Shah, I. Naharudin, T.W. Wong, In Vitro
696 Investigation of Influences of Chitosan Nanoparticles on Fluorescein Permeation
697 into Alveolar Macrophages, Pharm. Res. (2016) 1–12. doi:10.1007/s11095-016-

698 1893-5.
699 [13] I.M. El-sherbiny, H.D.C. Smyth, Controlled Release Pulmonary Administration of
700 Curcumin Using Swellable Biocompatible Microparticles, Mol Pharm. (2012).
701 [14] V.A. Fadok, D.R. Voelker, P.A. Campbell, J.J. Cohen, D.L. Bratton, P.M. Henson,
702 Exposure of phosphatidylserine on the surface of apoptotic lymphocytes triggers
703 specific recognition and removal by macrophages., J. Immunol. 148 (1992) 2207–
704 16. http://www.jimmunol.org/content/148/7/2207.abstract.
705 [15] D.P. Gaspar, V. Faria, L.M.D. Gonçalves, P. Taboada, C. Remuñán-López, A.J.
706 Almeida, Rifabutin-loaded solid lipid nanoparticles for inhaled antitubercular
707 therapy: Physicochemical and in vitro studies, Int. J. Pharm. 497 (2016) 199–209.
708 doi:10.1016/j.ijpharm.2015.11.050.
709 [16] T. Geelen, S.Y. Yeo, L.E.M. Paulis, L.W.E. Starmans, K. Nicolay, G.J. Strijkers,
710 Internalization of paramagnetic phosphatidylserine-containing liposomes by
711 macrophages, J. Nanobiotechnology. 10 (2012) 37. doi:10.1186/1477-3155-10-37.
712 [17] A. Gramatica, R.A. Petazzi, M.J. Lehmann, J. Ziomkowska, A. Herrmann, S.
713 Chiantia, ??Env-decorated phosphatidylserine liposomes trigger phagocytosis of
714 HIV-virus-like particles in macrophages, Nanomedicine Nanotechnology, Biol.
715 Med. 10 (2014) 981–989. doi:10.1016/j.nano.2014.02.008.
716 [18] K.R. Peterson, M.A. Cottam, A.J. Kennedy, A.H. Hasty, Macrophage-Targeted
717 Therapeutics for Metabolic Disease, Cell Press. 39 (2018) 536–546.
718 doi:10.1016/j.tips.2018.03.001.
719 [19] A. Costa, B. Sarmento, V. Seabra, Mannose-functionalized solid lipid
720 nanoparticles are e ff ective in targeting alveolar macrophages, Eur. J. Pharm. Sci.

114 (2018) 103–113. doi:10.1016/j.ejps.2017.12.006.

[20] E. Maretti, L. Costantino, C. Rustichelli, E. Leo, M. Antonietta, F. Buttini, E. Truzzi, V. Iannuccelli, Surface engineering of Solid Lipid Nanoparticle assemblies by methyl a - D -mannopyranoside for the active targeting to macrophages in anti-tuberculosis inhalation therapy, Int. J. Pharm. 528 (2017) 440–451. doi:10.1016/j.ijpharm.2017.06.045.

[21] L. Zou, Y. Tao, G. Payne, L. Do, T. Thomas, J. Rodriguez, H. Dou, Targeted delivery of nano-PTX to the brain tumor-associated macrophages, Oncotarget. (2016) 1–15.

[22] K. Binnemars-postma, G. Storm, J. Prakash, Nanomedicine Strategies to Target Tumor-Associated Macrophages, Int. J. Mol. Sci. 18 (2017) 1–27. doi:10.3390/ijms18050979.

[23] N. Mubin, M.S. Umar, S. Zubair, M. Owais, Selective Targeting of Functionalized Mycobacterium tuberculosis Protein Loaded Chitosan Nanoparticle to Macrophages : Correlation With Activation of Immune System, Front. Microbiol. 9 (2018) 1–15. doi:10.3389/fmicb.2018.02469.

[24] R.N. Lewis, R.N. McElhaney, Calorimetric and spectroscopic studies of the thermotropic phase behavior of lipid bilayer model membranes composed of a homologous series of linear saturated phosphatidylserines., Biophys. J. 79 (2000) 2043–2055. doi:10.1016/S0006-3495(00)76452-6.

[25] K. Segawa, S. Nagata, An Apoptotic “Eat Me” Signal: Phosphatidylserine Exposure, Trends Cell Biol. 25 (2015) 639–650. doi:10.1016/j.tcb.2015.08.003.

[26] F. Badalà, K. Nouri-mahdavi, D.A. Raoof, Apoptotic cell clearance: basic biology

and therapeutic potential, Nat Rev Immunol. 144 (2008) 724–732. doi:10.1038/jid.2014.371.

[27] M. Manrique-moreno, L. Heinbockel, M. Suwalsky, P. Garidel, K. Brandenburg, Biochimica et Biophysica Acta Biophysical study of the non-steroidal anti-in fl ammatory drugs (NSAID) ibuprofen , naproxen and diclofenac with phosphatidylserine bilayer membranes, BBA - Biomembr. 1858 (2016) 2123–2131. doi:10.1016/j.bbamem.2016.06.009.

[28] N. Joshi, T. Shanmugam, A. Kaviratna, R. Banerjee, Proapoptotic lipid nanovesicles: Synergism with paclitaxel in human lung adenocarcinoma A549 cells, J. Control. Release. 156 (2011) 413–420. doi:10.1016/j.jconrel.2011.07.025.

[29] H. Hosseini, Y. Li, P. Kanellakis, C. Tay, A. Cao, P. Tipping, A. Bobik, B.H. Toh, T. Kyaw, Phosphatidylserine liposomes mimic apoptotic cells to attenuate atherosclerosis by expanding polyreactive IgM producing B1a lymphocytes, Cardiovasc. Res. 106 (2015) 443–452. doi:10.1093/cvr/cvv037.

[30] Z. Wang, S.K. Gupta, S.A. Meenach, Development and physicochemical characterization of acetalated dextran aerosol particle systems for deep lung delivery, Int. J. Pharm. 525 (2017) 264–274. doi:10.1016/j.ijpharm.2017.04.052.

[31] Z. Wang, J.L. Cuddigan, S.K. Gupta, S.A. Meenach, Nanocomposite microparticles (nCmP) for the delivery of tacrolimus in the treatment of pulmonary arterial hypertension, Int. J. Pharm. 512 (2016) 305–313. doi:10.1016/j.ijpharm.2016.08.047.

[32] E.M. Bachelder, E.N. Pino, K.M. Ainslie, Acetalated Dextran: A Tunable and Acid-Labile Biopolymer with Facile Synthesis and a Range of Applications,

767 Chem. Rev. 117 (2017) 1915–1926. doi:10.1021/acs.chemrev.6b00532.
768 [33] K.E. Broaders, J. a Cohen, T.T. Beaudette, E.M. Bachelder, J.M.J. Fréchet,
769 Acetalated dextran is a chemically and biologically tunable material for particulate
770 immunotherapy., Proc. Natl. Acad. Sci. U. S. A. 106 (2009) 5497–502.
771 doi:10.1073/pnas.0901592106.
772 [34] E.M. Bachelder, T.T. Beaudette, K.E. Broaders, J. Dashe, J.M.J. Fréchet, Acetal-
773 derivatized dextran: An acid-responsive biodegradable material for therapeutic
774 applications, J. Am. Chem. Soc. 130 (2008) 10494–10495. doi:10.1021/ja803947s.
775 [35] S. a Meenach, Y.J. Kim, K.J. Kauffman, N. Kanthamneni, E.M. Bachelder, K.M.
776 Ainslie, Synthesis, Optimization, and Characterization of Camptothecin- Loaded
777 Acetalated Dextran Porous Microparticles for Pulmonary Delivery, Mol Pharm.
778 (2012). doi:10.1021/mp2003785.
779 [36] K.J. Peine, M. Guerau-De-Arellano, P. Lee, N. Kanthamneni, M. Severin, G.D.
780 Probst, H. Peng, Y. Yang, Z. Vangundy, T.L. Papenfuss, A.E. Lovett-Racke, E.M.
781 Bachelder, K.M. Ainslie, Treatment of experimental autoimmune
782 encephalomyelitis by codelivery of disease associated peptide and dexamethasone
783 in acetalated dextran microparticles, Mol. Pharm. 11 (2014) 828–835.
784 doi:10.1021/mp4005172.
785 [37] Z. Wang, S.A. Meenach, Synthesis and Characterization of Nanocomposite
786 Microparticles (nCmP) for the Treatment of Cystic Fibrosis-Related Infections,
787 Pharm. Res. (2016) 1–11. doi:10.1007/s11095-016-1921-5.
788 [38] A. Beloqui, R. Coco, P.B. Memvanga, B. Ucakar, A. Des Rieux, V. Préat, PH-
789 sensitive nanoparticles for colonic delivery of curcumin in inflammatory bowel

disease, Int. J. Pharm. 473 (2014) 203–212. doi:10.1016/j.ijpharm.2014.07.009.

[39] A. Kunwar, A. Barik, B. Mishra, K. Rathinasamy, R. Pandey, K.I. Priyadarsini, Quantitative cellular uptake, localization and cytotoxicity of curcumin in normal and tumor cells, Biochim. Biophys. Acta - Gen. Subj. 1780 (2008) 673–679. doi:10.1016/j.bbagen.2007.11.016.

[40] Y. Cong, L. Wang, A. Konrad, T. Schoeb, C.O. Elson, Curcumin induces the tolerogenic dendritic cell that promotes differentiation of intestine-protective regulatory T cells, Eur. J. Immunol. 39 (2009) 3134–3146. doi:10.1002/eji.200939052.

[41] S. Chanburee, W. Tiyaboonchai, Enhanced intestinal absorption of curcumin in Caco-2 cell monolayer using mucoadhesive nanostructured lipid carriers., J. Biomed. Mater. Res. B. Appl. Biomater. (2017) 1–8. doi:10.1002/jbm.b.33884.

[42] S. Tima, S. Anuchapreeda, C. Ampasavate, C. Berkland, S. Okonogi, Stable curcumin-loaded polymeric micellar formulation for enhancing cellular uptake and cytotoxicity to FLT3 overexpressing EoL-1 leukemic cells, Eur. J. Pharm. Biopharm. 114 (2017) 57–68. doi:10.1016/j.ejpb.2016.12.032.

[43] S.A. Malekar, A.L. Sarode, A.C. Bach, A. Bose, G. Bothun, D.R. Worthen, Radio Frequency-Activated Nanoliposomes for Controlled Combination Drug Delivery., AAPS PharmSciTech. 16 (2015) 1335–43. doi:10.1208/s12249-015-0323-z.

[44] S.A. Malekar, A.L. Sarode, A.C. Bach, D.R. Worthen, The Localization of Phenolic Compounds in Liposomal Bilayers and Their Effects on Surface Characteristics and Colloidal Stability., AAPS PharmSciTech. 17 (2016) in press. doi:10.1208/s12249-016-0483-5.

813 [45] L. Procházková, Y. Rodríguez-Muñoz, J. Procházka, J. Wanner, Simple
814 spectrophotometric method for determination of polyvinylalcohol in different
815 types of wastewater, Int. J. Environ. Anal. Chem. 94 (2014) 399–410.
816 doi:10.1080/03067319.2013.853761.
817 [46] J. Charles, M. Stewart, Colorimetric Determination of Phospholipids with
818 Ammonium Ferrothiocyanate, Anal. Biochem. 14 (1980) 10–14.
819 doi:10.1016/0003-2697(80)90269-9.
820 [47] J.W. Coleman, Nitric Oxide in Immunity and Inflammation, Int.
821 Immunopharmacol. 1 (2001) 1397–1406. doi:10.1016/j.neuroscience.2018.06.012.
822 [48] S.E.A. Gratton, P.A. Ropp, P.D. Pohlhaus, J.C. Luft, V.J. Madden, M.E. Napier,
823 J.M. Desimone, The effect of particle design on cellular internalization pathways,
824 Proc Natl Acad Sci U S A. 105 (2008).
825 [49] A. Albanese, P.S. Tang, W.C.W. Chan, The Effect of Nanoparticle Size , Shape ,
826 and Surface Chemistry on Biological Systems, Annu. Rev. Biomed. Eng. (2012).
827 doi:10.1146/annurev-bioeng-071811-150124.
828 [50] D.M.K. Jensen, D. Cun, M.J. Maltesen, S. Frokjaer, H.M. Nielsen, C. Foged,
829 Spray drying of siRNA-containing PLGA nanoparticles intended for inhalation, J.
830 Control. Release. 142 (2010) 138–145. doi:10.1016/j.jconrel.2009.10.010.
831 [51] S. Honary, F. Zahir, Effect of Zeta Potential on the Properties of Nano - Drug
832 Delivery Systems - A Review (Part 2), Trop. J. Pharm. Al Res. 12 (2013) 265–273.
833 doi:10.4314/tjpr.v12i2.19.
834 [52] S. Honary, F. Zahir, Effect of zeta potential on the properties of nano-drug
835 delivery systems - A review (Part 1), Trop. J. Pharm. Res. 12 (2013) 255–264.

836 doi:10.4314/tjpr.v12i2.19.
837 [53] J.G. Weers, D.P. Miller, Formulation Design of Dry Powders for Inhalation, J.
838 Pharm. Sci. 104 (2015) 3259–3288. doi:10.1002/jps.24574.
839 [54] R.P. Barroso, L.G.M. Basso, A.J. Costa-filho, Interactions of the antimalarial
840 amodiaquine with lipid model membranes, Chem. Phys. Lipids. 186 (2015) 68–78.
841 doi:10.1016/j.chemphyslip.2014.12.003.
842 [55] R.H. Fang, S. Aryal, C.M.J. Hu, L. Zhang, Quick synthesis of lipid-polymer
843 hybrid nanoparticles with low polydispersity using a single-step sonication
844 method, Langmuir. 26 (2010) 16958–16962. doi:10.1021/la103576a.
845 [56] E. Maretti, T. Rossi, M. Bondi, M.A. Croce, M. Hanuskova, E. Leo, F. Sacchetti,
846 V. Iannuccelli, Inhaled Solid Lipid Microparticles to target alveolar macrophages
847 for tuberculosis, Int. J. Pharm. 462 (2014) 74–82.
848 doi:10.1016/j.ijpharm.2013.12.034.
849